ACS APPLIED POLYMER MATERIALS

Forum Article

Cite This: ACS Appl. Polym. Mater. 2020, 2, 91−97

pubs.acs.org/acsapm

Effects of Side Chain on High Temperature Operation Stability of Conjugated Polymers

Dung T. Tran,[†] Aristide Gumyusenge,[†] Xuyi Luo,[†] Michael Roders,[‡] Zhengran Yi,[†] Alexander L. Ayzner,[‡] and Jianguo Mei*[,†]

[†]Department of Chemistry, Purdue University, West Lafayette, Indiana 47907, United States

[‡]Department of Chemistry and Biochemistry, University of California at Santa Cruz, 1156 High Street, Santa Cruz, California 95064, United States

Supporting Information

ABSTRACT: Understanding high-temperature operation in organic semiconductors remains elusive. Here, we studied the effect of two alkyl side-chains, 2-octyldodecyl (C1) and 4-decyltetracecyl (C3), on the thermal stability of two types of conjugated polymer backbones: isoindigo (IID) and diketopyrolopyrrole (DPP). All polymers remain functional with high on/off ratio in ambient air at temperature up to 220 °C. However, the use of longer side-chain C3 lowers the $\pi-\pi$ stacking distance and enables more thermally stable polymer thin film field-effect-transistors. Specifically, IID-C3 and DPP-C3 exhibited less alteration in threshold voltage as well as a reduction in effective mobility at high temperature. This behavior emphasizes the importance of close $\pi-\pi$ stacking distance on charge transport properties of conjugated polymers and their thermal stability. This study is a starting point to deconvolute the intricate mechanism of charge transport in polymer thin films at elevated temperatures.

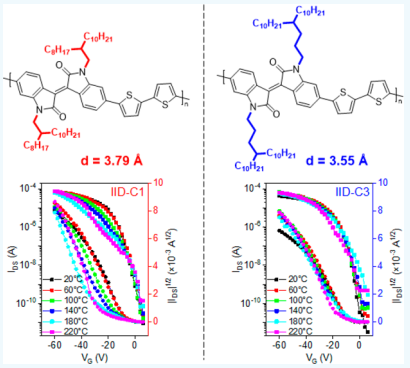

KEYWORDS: *high-temperature electronics, thermal stability, side chain, OFET, contact resistance*

1. INTRODUCTION

Electronic devices capable of functioning in high-temperature environments are of great interest for many industries such as automotive- and aeroengineering. The development of high-temperature semiconductors has thus attracted close attention. Inorganic wide band gap semiconductors such as SiC and GaN have been the focus as they can potentially operate at temperatures up to 300−400 °C.[1−3] Their expensive and complicated processing conditions, unfortunately, hinder them from a wide adoption.[4] At the same time, organic semiconductors are lightweight and can be solution-processed, which is both much cheaper and more accessible, especially for large area fabrication.[5] These advantages make them useful for applications requiring cost-effective, lightweight materials, where any additional weight matters such as aerospace. However, studies about organic semiconductors thermal stability are rare, especially with *in situ* electrical measurements at temperature above 100 °C,[6,7] and their thermal stability is mostly unimpressive. The charge carrier mobilities of organic semiconductors quickly deteriorate at temperature higher than 150 °C.[8−12] In the case of small molecules, the reasons are attributed to the structural instability of the molecule[8−11] and the increase of trapping sites at the dielectric−semiconductor interface.[13] For conjugated polymers, P3HT shows a sharp degradation of mobility when the temperature is getting above 150 °C. In this case, the performance deterioration is caused by the twisted backbone and the decline of the conjugation length.[12] In one of a few successful attempts of creating a functional OFET device at elevated temperature, Seifrid et al.[14] reported a high melting point small molecule organic semiconductor that can operate at 200 °C and survive after three heating−cooling cycles. With semiconducting polymers, to the best of our knowledge, we have not had a systematic study about structure−thermal stability relationship of pure conjugated polymers. Recently, our group proposed a universal strategy applying to a wide range of different conjugated polymers: the blends with a high glass transition temperature (T_g) insulating matrix.[15,16] We found that with proper control of ratio and proper selection of the blending pair, the blends exhibit stable charge transport at up to 220 °C. We believe that one of the key contributing factors of the improved high-temperature stability is the shorter $\pi-\pi$ stacking distance between semiconducting polymer chains in the blends compared to the pure polymers. This spatial confinement between polymer chains reduces the dihedral angle rotation in the backbone and restricts the conformational twisting movement, which is harmful to the charge transport. In this paper, we provide more evidence of the effect of $\pi-\pi$ intermolecular interactions on the thermal stability using

Special Issue: Young Investigator Forum

Received: October 22, 2019
Accepted: November 27, 2019
Published: December 11, 2019

DOI: 10.1021/acsapm.9b00999
ACS Appl. Polym. Mater. 2020, 2, 91−97

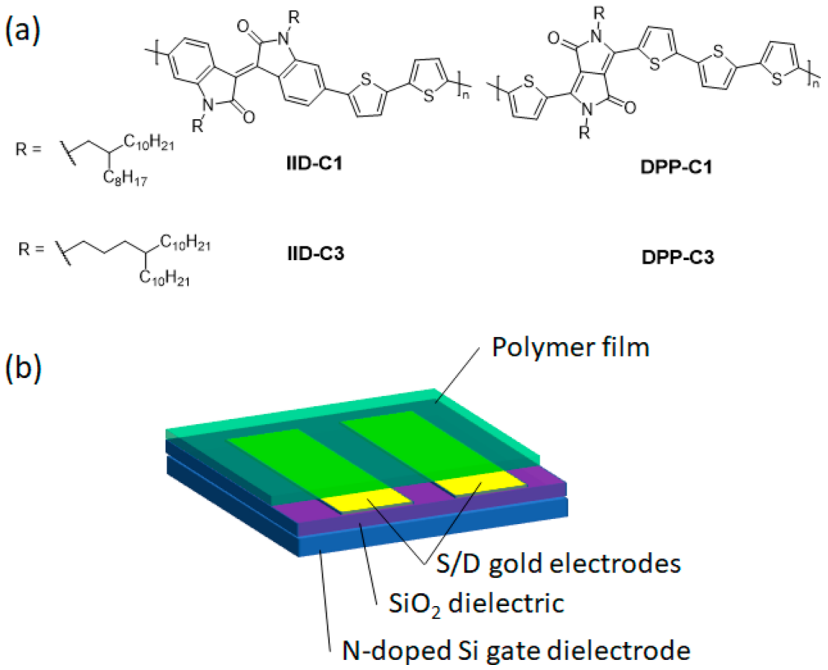

Figure 1. (a) Chemical structures of IID- and DPP-based polymers. (b) Illustration of bottom-gate bottom-contact devices used in this work. The channel length is 100 μm, and the channel width is 1000 μm.

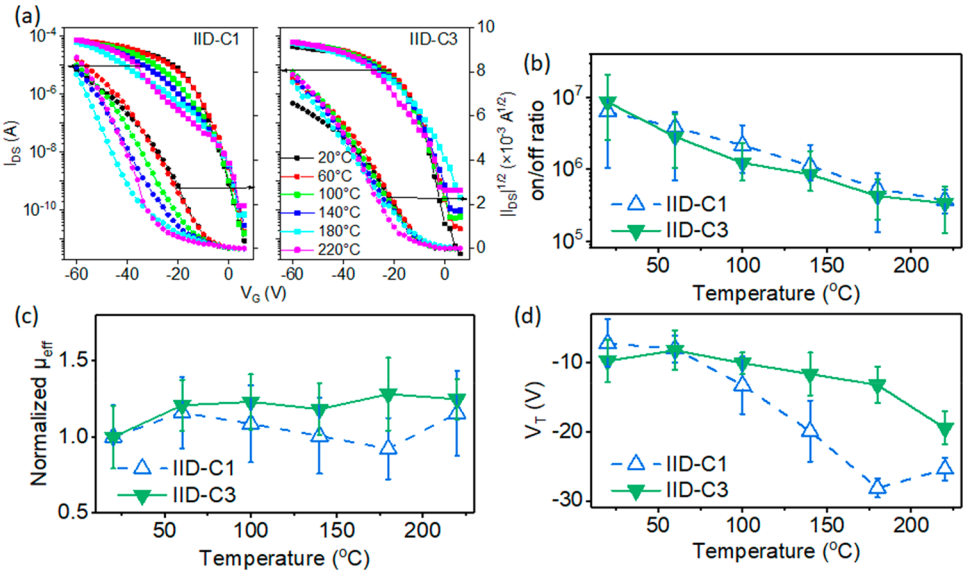

Figure 2. (a) Typical transfer curves of IID-C1 and IID-C3. (b) Average on/off ratio. (c) Average normalized μ_{eff} to the μ_{eff} at room temperature. (d) Average V_T shift extracted from 10 different devices of each polymer from room temperature to 220 °C.

conjugated polymers with different $\pi-\pi$ stacking distance by tuning their branching alkyl side chain. The branched alkyl position usually is moved further away from the backbone to shorten the $\pi-\pi$ stacking distance of the polymer chains, aiming to improve the charge mobility of the polymers at room temperature.[17−20] Lei et al.[18] showed that moving the side chain further than three carbons does not reduce the $\pi-\pi$ stacking distance or benefit the performance for isoindigo-based polymers.

Herein, we investigate the effect of changing the branching position of the solubilizing alkyl side chains from one (2-octyldodecyl (C1)) to three (4-decyltetracecyl (C3)) methylene units on the thermal stability of two very common sets of backbone, isoindigo (IID) and diketopyrrolopyrrole (DPP) (Figure 1a). We employed *in situ* temperature-dependent diffraction scanning, UV−vis absorption analysis, and contact resistance measurements to show that, in both cases, the C3 polymers, with smaller $\pi-\pi$ stacking distances, display a relatively more stable transfer characteristic at high temperature compared to their C1 polymers counterparts.

2. RESULTS AND DISCUSSION

First, we studied the *in situ* temperature-dependent charge transport behavior of all of the polymers from room temperature to 220 °C in ambient air. Bottom gate bottom contact (BGBC) thin film field effect transistors were used. The channel width (W) and length (L) were 1000 and 100 μm, respectively (Figure 1b). All polymers in comparison were

DOI: 10.1021/acsapm.9b00999
ACS Appl. Polym. Mater. 2020, 2, 91−97

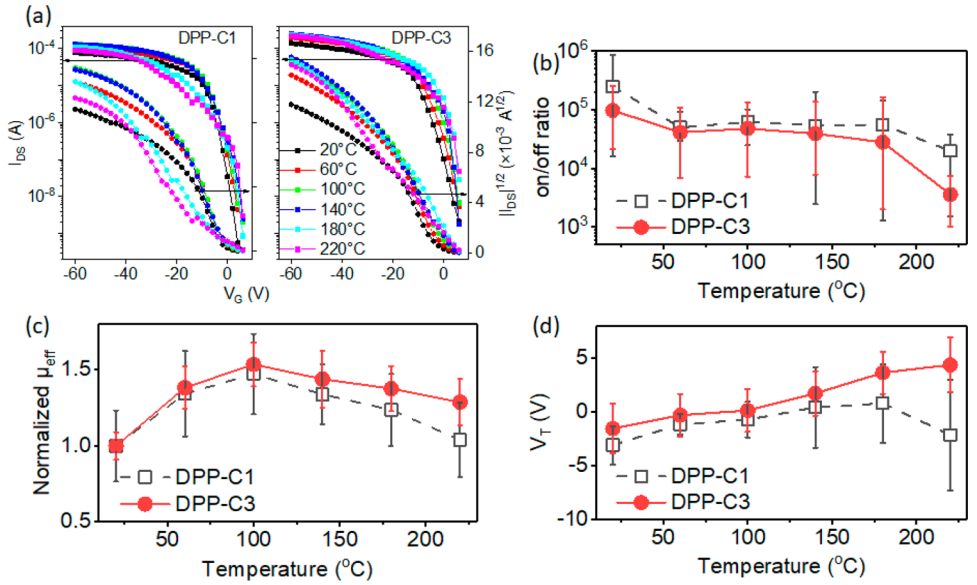

Figure 3. (a) Typical transfer curves of DPP-C1 and DPP-C3. (b) Average on/off ratio. (c) Average normalized μ_{eff} to the μ_{eff} at room temperature. (d) Average V_T shift extracted from 10 different devices of each polymer from room temperature to 220 °C.

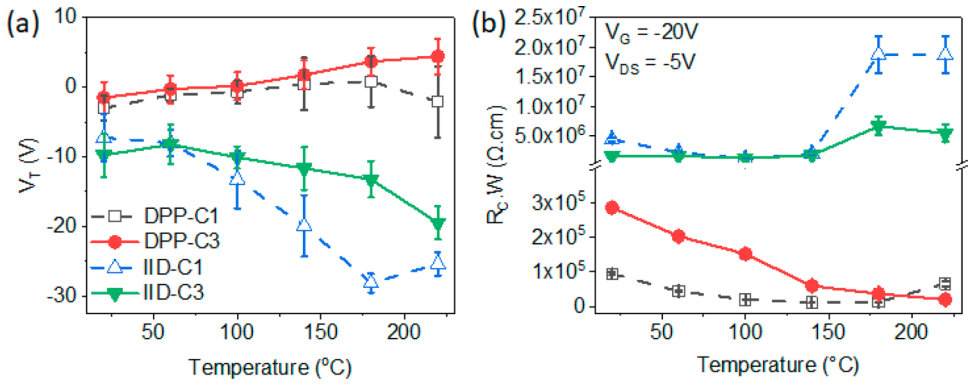

Figure 4. (a) Average threshold voltage (V_T). (b) Contact resistance, at $V_G = -20$ V, of all four conjugated polymers at different temperatures from 20 to 220 °C.

prepared and processed in the same condition, as described in the Experimental Section. Usually, mobility μ, which is calculated from the equation $I_{DS} = (\mu WC/2L)(V_G - V_T)$,[2] is used as the benchmark of the performance of semiconductor. However, we do not use it for this study because the polymers transfer curves are not perfectly "ideal" and they change shapes at different temperature. Nonideal curves might lead to severe overestimation or underestimation of the real mobility.[21,22] Hence, we consider a polymer qualitatively "more stable" than the other if its transfer curves at high temperature overlap better with those at lower temperature. Quantitatively, higher stability means less change in threshold voltage (V_T) and effective mobility (μ_{eff}).[21] The extracting methods of these two parameters and the average μ_{eff} of these polymers are detailed in the Supporting Information (Figures S1−S5).

There are noticeable differences between the transfer curves of these two isoindigo polymers (Figure 1a). In general, both polymers remain functional at up to 220 °C (Figure 2a). As temperature increases, the IID polymers display a decrease in on/off ratio (still above 10^5 at 220 °C) due to thermally activated hopping transport[14] and a negative V_T shift (Figure 2b,d). However, in IID-C1, the extent of change is much more significant than that in IID-C3. From 60 to 220 °C, IID-C1 shows a gradual decline in μ_{eff} and a significant shift of V_T from about −8 V to −30 V, while IID-C3 can retain relatively stable on-current and threshold voltage (Figure 2c,d). This polymer μ_{eff} remains almost unchanged after 60 °C, and its V_T only shifts in the range of 10 V compared to more than 20 V for IID-C1.

DPP-polymers show a similar trend with the IID polymer pair as the DPP-C3 is more stable than DPP-C1 at high temperature, even though the difference is not as significant as in the IID pair. Two DPP polymers behave very similarly at temperature up to 140 °C. They both observe the decrease of on/off ratio (Figure 3a,b), the increase of μ_{eff} (Figure 3c), and the V_T shift to the positive voltage (Figure 3d). After 140 °C, both polymers witness the gradual decrease in μ_{eff}, but DPP-C1 reduces slightly more noticeably (Figure 3c). The difference also can be noticed in terms of V_T shifting. While V_T of DPP-C3 continues moving to the positive region at above 180 °C, similar to the behavior of inorganic materials,[2] DPP-C1 threshold voltage shifts toward the gate bias and its transfer curves change to nonideal S-shape.

The most noticeable discrepancy in these four polymers is the threshold voltage shifting at high temperature region, especially above 180 °C (Figure 4a). In all cases, as the

DOI: 10.1021/acsapm.9b00999
ACS Appl. Polym. Mater. 2020, 2, 91−97

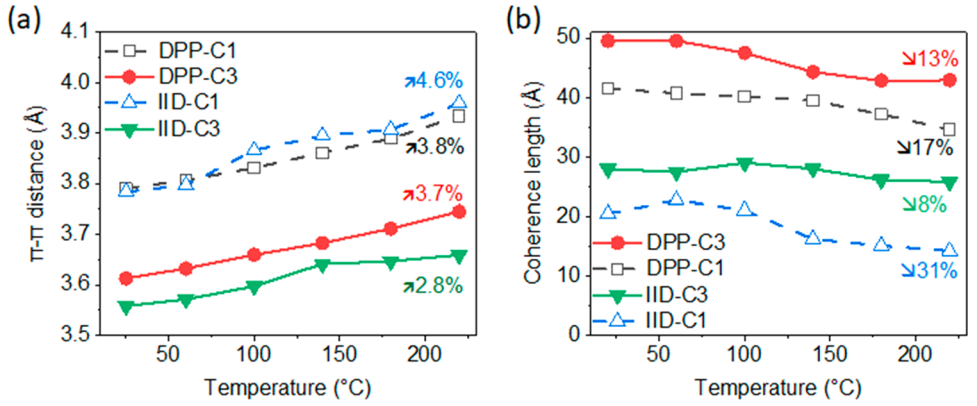

Figure 5. Expansion of(a) $\pi-\pi$ stacking distance and (b) temperature-dependent coherence length of all four polymers from room temperature to 220 °C. The numbers indicate how much the polymer films changed in the (a) in-plane direction and (b) coherence length, respectively.

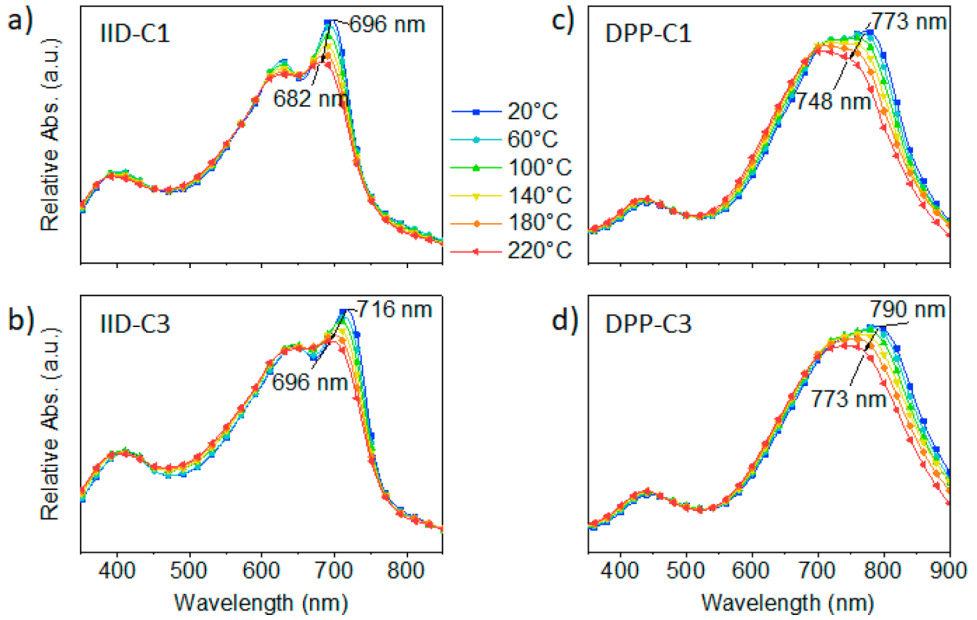

Figure 6. *In situ* temperature-dependent UV–vis/NIR absorption spectra of (a, b) IID polymers and (c, d) DPP polymers.

temperature increases, the V_T first shifts to the positive side, which was already reported in several organic semiconductors in lower temperature range.[23] A possible explanation is that as the temperature increase, charge carriers gain enough thermal energy to be activated and jump into the transport level without the need for applied gate voltage. As a result, the off-current arises, and the V_T shifts to the positive side. However, at higher temperature, the threshold voltage shifts back to the opposite direction. This is possibly because elevated temperature triggers the twisting backbone, degrades both intrachain and interchain charge transport, and creates more traps on the charge conductive pathway.[24] The effect of bias stress[25] on this threshold voltage shift is ruled out because all of the devices were scanned multiple times after a 30 s interval, and no significant change was observed after two scans. Another factor that contributes to the threshold voltage shifting is charge injection from metal/semiconductor interface. Liu et al. demonstrated that high contact resistance could decrease the on-current and shift the V_T to the negative side for p-type disordered semiconductor.[26] To test the development of contact resistance at different temperatures, we employed the modified transmission line method (m-TLM)[27] (Figure 4b). All four polymers witnessed the gradual decrease of contact resistance at temperature up to 100 °C. This phenomenon agrees with the observation that contact resistance is a thermally activated process at low-temperature region.[28] However, in two IID-polymers, which suffer the most from the variation of V_T, their contact resistance takes off after the temperature reach 180 °C. Notably, the R_C increase of IID-C1 was significantly higher than that of IID-C3, which possibly explained the larger V_T shift of IID-C1 at high temperature. For both DPP polymers, they have relatively lower contact resistance, and it reflects into the more stable threshold voltage of these polymers compared to their isoindigo counterparts as well as higher mobility enhancement. DPP-C3 contact resistance shows a monotonous descending trend, while that of DPP-C1 starts to go back up at 180 °C. This phenomenon explains the negative shifting of V_T of DPP-C1 from 180 °C. In general, high contact resistance could affect the behaviors of semiconducting polymers at high temperature.

To elucidate the observed behaviors of these polymers, *in situ* temperature-dependent GIXRD and UV–vis/NIR absorption are used to investigate their intermolecular interaction properties. The GIXRD data agree well with the trends

DOI: 10.1021/acsapm.9b00999
ACS Appl. Polym. Mater. 2020, 2, 91–97

reported elsewhere,[15,18,29] in which the $\pi-\pi$ stacking distances of C1-polymers are larger than those of their C3 counterparts. In all cases, due to the thermal expansion, both $\pi-\pi$ stacking and lamellar packing distance increase with temperature. While the IID-C1 $\pi-\pi$ stacking distance increases by 4.8% from 3.78 to 3.96 Å, that of IID-C3 increases only 2.8% from 3.56 to 3.66 Å, which is still shorter than the original $\pi-\pi$ stacking distance of IID-C1 at room temperature (Figure 5a). In the lamellar direction, IID-C1 expands by almost 9%, while IID-C3 lamellar distance only rises by 6%. In terms of coherence length, IID-C1 also exhibits more significant alteration than its corresponding IID-C3. Specifically, the coherence length of IID-C1 decreases by 31%, from 2 nm to only 1.4 nm at 220 °C. At the same time, IID-C3 crystal coherence length decreases by only 8% (Figure 5b). Longer coherence length polymers usually corelates with larger crystallite, fewer grain boundaries, and thus results in higher charge transport mobility.[30] In summary, the IID-C1 crystalline domain alters more significantly upon heating than IID-C3, which correlates to the more substantial change in charge transport, accompanying with higher contact resistance raise. For DPP polymer pair, the difference in their $\pi-\pi$ stacking distance is smaller than that of IID polymers. Also, the fact that both DPP polymers expanded on a similar scale (Figure 5a,b) partly explains the more subtle difference of this polymer pair's thermal stability compared to their IID polymers.

In the temperature-dependent UV−vis/NIR absorption spectra (Figure 6), both types of polymer displayed the dual-band absorption of donor−acceptor polymer semiconductors. At room temperature, compared to C1 polymers, both C3 polymers show a red-shifted absorption of the (0−0) and (0−1) peaks by about 20 nm. The more red-shifted absorption peak usually is attributed to a better backbone coplanarity. As the temperature increases, both peaks blue-shift by about 20 nm for IID polymers and 15 nm for DPP polymers, while the peak intensity decreases. This phenomenon is correlated with the reduction of interchain interaction as well as the twisted backbone of these polymers at high temperature.[15]

The UV−vis and GIXRD results suggest that both C3 polymers have closer $\pi-\pi$ stacking distance and more planar backbone than C1 polymers at both low and high temperatures. According to our molecular dynamic simulation in our previous study,[15] smaller $\pi-\pi$ stacking distance will reduce the thermal fluctuation of the backbone, the dynamic disorder, and therefore abate the charge scattering as well as trapping on the charge transport pathways. This effect explains the fact that both C3 polymers can retain higher effective mobility as well as more stable threshold voltage at high temperature compared to their C1 counterparts. In addition, two DPP polymers show a similar extent of thermal expansion, while there is a distinct difference between the IID polymer pair. In the same temperature range, IID-C1 expands more considerably than IID-C3, especially in in-plane $\pi-\pi$ stacking direction (4.6% and 2.8%, respectively). The more considerable difference in thermal mismatch and thermal expansion of the IID pair results in the larger difference in their thermal stability compared to that of the DPP pair.

3. CONCLUSIONS

In conclusion, we investigated the effect of different branching side-chain positions on the thermal stability of two sets of conjugated IID- and DPP-based polymers. In all cases, moving the branching side chain further away from the backbone and the use of longer side chain make more thermally stable polymers. Specifically, C3 side chain helps to lower the $\pi-\pi$ stacking distance and improve the coplanarity of the backbone, which reduces the dynamic disorder of the charge transport of conjugated polymers. Also, C3 polymers display smaller contact resistance than their C1 counterparts that leads to a more stable threshold voltage at high temperature. We believe achieving high thermal stable conjugated polymer thin film transistor could come from both molecular design and device engineering. More systematic studies about the effect of polymer structure such as the molecular weight, polymer backbones, or factors of the devices such as device architecture or contact resistance will be conducted in the future to disclose the mystery of charge transport in conjugated polymers at high temperature.

4. EXPERIMENTAL SECTION

4.1. Materials. All IID-C1, IID-C3, DPP-C1, and DPP-C3 were synthesized and purified as reported in the previous works.[18,31,32] The molecular weights and polydispersity index (PDI) were evaluated by high-temperature gel permeation chromatography (GPC): IID-C1 (M_n = 20k; PDI = 3.8); IID-C3 (M_n= 32k, PDI = 3.2); DPP-C1 (M_n = 52k; PDI = 4.3); and DPP-C3 (M_n = 52k; PDI = 4.5).

4.2. OFET Devices Fabrication and Characterization. A heavily n-doped Si wafer with a 300 nm SiO_2 surface dielectric layer (capacitance of 11.5nF/cm^2) was used as the substrate. The gold source and drain electrodes were sputtered and patterned by photolithography technique. For the octadecyltrichlorosilane (OTS) modification, the silicon wafer was first cleaned with hot piranha solution (98% H_2SO_4/30% H_2O_2 = 7:3). It was followed by sonicating in water, isopropanol, and acetone sequentially for 5 min each. After drying in an oven, the silicon wafer was placed in a Petri dish with a tiny drop of OTS. The dish was covered and put in a vacuum oven at 120 °C for 3 h to form an OTS self-assembled monolayer on the surface. The OTS modified substrates were rinsed successively with hexane, isopropanol, and chloroform and dried by nitrogen before use. All polymers were dissolved in chloroform at 10 mg/mL at 50 °C for 1 h until completely dissolved. The solution was then spin-coated in ambient air with the speed of 2000 rpm for 30 s to obtain the film thickness of 80−100 nm. The devices were annealed in an N_2 glovebox at 220 °C and then slowly cooled down to 25 °C before measurements.

OFET characterizations were carried out using a Keithley 4200 in ambient condition. OFET performances were obtained by applying a gate bias from 6 V to −60 V, with the source−drain voltage at −60 V. The threshold voltage was determined, as illustrated in Figures S2−S5. To control the temperature, the HFS600E-PB4 Linkam stage was used. The heating rate was maintained at 10 °C/min and increased from 20 to 220 °C in steps of 40 °C for all characterizations.

4.3. Temperature-Dependent UV−vis Spectroscopy. Samples were prepared by spin coating the polymer solutions onto cleaned glass slides then was mounted inside the HFS600E-PB4 Linkam stage. The stage then was brought into the light path inside the UV−vis/NIR Cary 3000i spectrophotometer. The baseline of the UV−vis needed to be taken at different temperature by using a cleaned glass slide inside the Linkam stage. Temperature-dependent spectra were then obtained with corresponding baseline correction.

DOI: 10.1021/acsapm.9b00999
ACS Appl. Polym. Mater. 2020, 2, 91−97

4.4. Contact Resistance Measurement. The contact resistances of these polymers were evaluated using modified transmission-line method reported elsewhere.[27] The channel lengths, L, were 5, 10, 20, 30, 40, 60, 80, and 100 μm. The channel width was kept at 1000 μm. The total resistance was calculated from the slope of the output curves in the linear region. The polymer thin films were prepared as the same procedure stated above.

4.5. Morphology Analysis. The AFM height images were obtained on a Veeco dimension 3100 atomic force microscope in tapping mode. The film was prepared by spin coating the solution on the OTS modified substrates. The film was annealed at 80 °C for 5 min to remove all solvent residual and then used to analyze the film morphology. Then the same films were annealed at 220 °C for 10 min and imaged at almost the same spots to obtain the morphology at high temperature.

■ ASSOCIATED CONTENT

Supporting Information

The Supporting Information is available free of charge at https://pubs.acs.org/doi/10.1021/acsapm.9b00999.

Effective mobility extraction, transistor characteristics, temperature-dependent AFM images, temperature-dependent 2D and 1D GIXRD pattern, contact resistance of all polymers (PDF)

■ AUTHOR INFORMATION

Corresponding Author

*E-mail: jgmei@purdue.edu.

ORCID

Alexander L. Ayzner: 0000-0002-6549-4721

Jianguo Mei: 0000-0002-5743-2715

Funding

This work was supported by the Office of Naval Research Young Investigator Program (ONR YIP Award, Nos. N00014−16−1−2551 and N00014−19−1−2027).

Notes

The authors declare no competing financial interest.

■ ABBREVIATIONS

IID, isoindigo; DPP, diketopyrrolopyrole; GIXRD, grazing incidence X-ray diffraction

■ REFERENCES

(1) Chalker, P. R. Wide Bandgap Semiconductor Materials for High Temperature Electronics. *Thin Solid Films* **1999**, *343−344* (1−2), 616−622.

(2) Neudeck, P.G.; Okojie, R.S.; Liang-Yu Chen. High-Temperature Electronics - a Role for Wide Bandgap Semiconductors? *Proc. IEEE* **2002**, *90* (6), 1065−1076.

(3) Dreike, P. L.; Fleetwood, D. M.; King, D. B.; Sprauer, D. C.; Zipperian, T. E. An Overview of High-Temperature Electronic Device Technologies and Potential Applications. *IEEE Trans. Compon., Packag., Manuf. Technol., Part A* **1994**, *17* (4), 594−609.

(4) Garrido-Diez, D.; Baraia, I. Review of Wide Bandgap Materials and Their Impact in New Power Devices. In *2017 IEEE International Workshop of Electronics, Control, Measurement, Signals and their Application to Mechatronics (ECMSM)*; IEEE, 2017; pp 1−6.

(5) Sirringhaus, H. 25th Anniversary Article: Organic Field-Effect Transistors: The Path beyond Amorphous Silicon. *Adv. Mater.* **2014**, *26* (9), 1319−1335.

(6) Liu, C.; Huang, K.; Park, W.-T.; Li, M.; Yang, T.; Liu, X.; Liang, L.; Minari, T.; Noh, Y.-Y. A Unified Understanding of Charge Transport in Organic Semiconductors: The Importance of Attenuated Delocalization for the Carriers. *Mater. Horiz.* **2017**, *4* (4), 608−618.

(7) Zhao, Y.; Zhao, X.; Roders, M.; Gumyusenge, A.; Ayzner, A. L.; Mei, J. Melt-Processing of Complementary Semiconducting Polymer Blends for High Performance Organic Transistors. *Adv. Mater.* **2017**, *29*, 1605056.

(8) Kato, Y.; Iba, S.; Teramoto, R.; Sekitani, T.; Someya, T.; Kawaguchi, H.; Sakurai, T. High Mobility of Pentacene Field-Effect Transistors with Polyimide Gate Dielectric Layers. *Appl. Phys. Lett.* **2004**, *84* (19), 3789−3791.

(9) Fan, Z.-P.; Li, X.-Y.; Purdum, G. E.; Hu, C.-X.; Fei, X.; Shi, Z.-F.; Sun, C.-L.; Shao, X.; Loo, Y.-L.; Zhang, H.-L. Enhancing the Thermal Stability of Organic Field-Effect Transistors by Electrostatically Interlocked 2D Molecular Packing. *Chem. Mater.* **2018**, *30* (11), 3638−3642.

(10) Dong, Y.; Guo, Y.; Zhang, H.; Shi, Y.; Zhang, J.; Li, H.; Liu, J.; Lu, X.; Yi, Y.; Li, T.; Hu, W.; Jiang, L. Cyclohexyl-Substituted Anthracene Derivatives for High Thermal Stability Organic Semiconductors. *Front. Chem.* **2019**, *7*, 11.

(11) Sekitani, T.; Iba, S.; Kato, Y.; Someya, T. Pentacene Field-Effect Transistors on Plastic Films Operating at High Temperature above 100°C. *Appl. Phys. Lett.* **2004**, *85* (17), 3902−3904.

(12) Joshi, S.; Pingel, P.; Grigorian, S.; Panzner, T.; Pietsch, U.; Neher, D.; Forster, M.; Scherf, U. Bimodal Temperature Behavior of Structure and Mobility in High Molecular Weight P3HT Thin Films. *Macromolecules* **2009**, *42* (13), 4651−4660.

(13) Vladimirov, I.; Müller, S.; Baumann, R.; Geßner, T.; Molla, Z.; Grigorian, S.; Köhler, A.; Bässler, H.; Pietsch, U.; Weitz, R. T. Dielectric-Semiconductor Interface Limits Charge Carrier Motion at Elevated Temperatures and Large Carrier Densities in a High-Mobility Organic Semiconductor. *Adv. Funct. Mater.* **2019**, *29* (12), 1807867.

(14) Seifrid, M.; Ford, M. J.; Li, M.; Koh, K. M.; Trefonas, P.; Bazan, G. C. Electrical Performance of a Molecular Organic Semiconductor under Thermal Stress. *Adv. Mater.* **2017**, *29* (12), 1605511.

(15) Gumyusenge, A.; Tran, D. T.; Luo, X.; Pitch, G. M.; Zhao, Y.; Jenkins, K. A.; Dunn, T. J.; Ayzner, A. L.; Savoie, B. M.; Mei, J. Semiconducting Polymer Blends That Exhibit Stable Charge Transport at High Temperatures. *Science (Washington, DC, U. S.)* **2018**, *362* (6419), 1131−1134.

(16) Gumyusenge, A.; Luo, X.; Ke, Z.; Tran, D. T.; Mei, J. Polyimide-Based High-Temperature Plastic Electronics. *ACS Mater. Lett.* **2019**, *1* (1), 154−157.

(17) Kawabata, K.; Saito, M.; Takemura, N.; Osaka, I.; Takimiya, K. Effects of Branching Position of Alkyl Side Chains on Ordering Structure and Charge Transport Property in Thienothiophenedione- and Quinacridone-Based Semiconducting Polymers. *Polym. J.* **2017**, *49* (1), 169−176.

(18) Lei, T.; Dou, J.-H.; Pei, J. Influence of Alkyl Chain Branching Positions on the Hole Mobilities of Polymer Thin-Film Transistors. *Adv. Mater.* **2012**, *24* (48), 6457−6461.

(19) Kang, I.; Yun, H.-J.; Chung, D. S.; Kwon, S.-K.; Kim, Y.-H. Record High Hole Mobility in Polymer Semiconductors via Side-Chain Engineering. *J. Am. Chem. Soc.* **2013**, *135* (40), 14896−14899.

(20) Bridges, C. R.; Ford, M. J.; Thomas, E. M.; Gomez, C.; Bazan, G. C.; Segalman, R. A. Effects of Side Chain Branch Point on Self Assembly, Structure, and Electronic Properties of High Mobility Semiconducting Polymers. *Macromolecules* **2018**, *51* (21), 8597−8604.

(21) Choi, H. H.; Cho, K.; Frisbie, C. D.; Sirringhaus, H.; Podzorov, V. Critical Assessment of Charge Mobility Extraction in FETs. *Nat. Mater.* **2018**, *17* (1), 2−7.

(22) Bittle, E. G.; Basham, J. I.; Jackson, T. N.; Jurchescu, O. D.; Gundlach, D. J. Mobility Overestimation Due to Gated Contacts in Organic Field-Effect Transistors. *Nat. Commun.* **2016**, *7* (1), 10908.

(23) Letizia, J. A.; Rivnay, J.; Facchetti, A.; Ratner, M. A.; Marks, T. J. Variable Temperature Mobility Analysis of N-Channel, p-Channel and Ambipolar Organic Field-Effect Transistors. *Adv. Funct. Mater.* **2010**, *20* (1), 50−58.

DOI: 10.1021/acsapm.9b00999
ACS Appl. Polym. Mater. 2020, 2, 91−97

(24) Häusermann, R.; Willa, K.; Blülle, B.; Morf, T.; Facchetti, A.; Chen, Z.; Lee, J.; Batlogg, B. Device Performance and Density of Trap States of Organic and Inorganic Field-Effect Transistors. *Org. Electron.* **2016**, *28*, 306−313.
(25) Phan, H.; Wang, M.; Bazan, G. C.; Nguyen, T. Q. Electrical Instability Induced by Electron Trapping in Low-Bandgap Donor-Acceptor Polymer Field-Effect Transistors. *Adv. Mater.* **2015**, *27* (43), 7004−7009.
(26) Liu, C.; Li, G.; Di Pietro, R.; Huang, J.; Noh, Y.-Y.; Liu, X.; Minari, T. Device Physics of Contact Issues for the Overestimation and Underestimation of Carrier Mobility in Field-Effect Transistors. *Phys. Rev. Appl.* **2017**, *8* (3), 034020.
(27) Xu, Y.; Gwoziecki, R.; Chartier, I.; Coppard, R.; Balestra, F.; Ghibaudo, G. Modified Transmission-Line Method for Contact Resistance Extraction in Organic Field-Effect Transistors. *Appl. Phys. Lett.* **2010**, *97* (6), 063302.
(28) Pesavento, P. V.; Chesterfield, R. J.; Newman, C. R.; Frisbie, C. D. Gated Four-Probe Measurements on Pentacene Thin-Film Transistors: Contact Resistance as a Function of Gate Voltage and Temperature. *J. Appl. Phys.* **2004**, *96* (12), 7312−7324.
(29) Zhang, X.; Richter, L. J.; DeLongchamp, D. M.; Kline, R. J.; Hammond, M. R.; McCulloch, I.; Heeney, M.; Ashraf, R. S.; Smith, J. N.; Anthopoulos, T. D.; Schroeder, B.; Geerts, Y. H.; Fischer, D. A.; Toney, M. F. Molecular Packing of High-Mobility Diketo Pyrrolo-Pyrrole Polymer Semiconductors with Branched Alkyl Side Chains. *J. Am. Chem. Soc.* **2011**, *133* (38), 15073−15084.
(30) Mazzio, K. A.; Rice, A. H.; Durban, M. M.; Luscombe, C. K. Effect of Regioregularity on Charge Transport and Structural and Excitonic Coherence in Poly(3-Hexylthiophene) Nanowires. *J. Phys. Chem. C* **2015**, *119* (27), 14911−14918.
(31) Li, Y.; Sonar, P.; Singh, S. P.; Soh, M. S.; Van Meurs, M.; Tan, J. Annealing-Free High-Mobility Diketopyrrolopyrrole-Quaterthiophene Copolymer for Solution-Processed Organic Thin Film Transistors. *J. Am. Chem. Soc.* **2011**, *133* (7), 2198−2204.
(32) Zhao, Y.; Zhao, X.; Zang, Y.; Di, C. A.; Diao, Y.; Mei, J. Conjugation-Break Spacers in Semiconducting Polymers: Impact on Polymer Processability and Charge Transport Properties. *Macromolecules* **2015**, *48* (7), 2048−2053.

DOI: 10.1021/acsapm.9b00999
ACS Appl. Polym. Mater. 2020, 2, 91−97